

Effect of Boundary Conditions on Freezing in Porous Media

Rahul Basu

Gas Turbine Research Establishment, Bangalore-56Q 093

ABSTRACT

This paper examines a model for coupled heat and mass transfer for freezing in a porous media with Dirichlet and convective boundary conditions. Variables include porosity, heat transfer coefficients, thermal and mass diffusivity, density, latent heat, and boundary temperatures. A simulation for the slab illustrates the appearance of undercooling. A stability criterion for the phase interface is linked with well-known metallurgical parameters like undercooling and freezing rate. A possible mechanism for freckling in ingots of niobium-rich superalloys is examined. It has been shown that heat and mass transfer balance at the interface can affect stability. The effect of boundary conditions on the velocity of freezing is computed for some cases, including the self-freezing process.

Keywords: Heat and mass transfer, boundary conditions, phase interface, advanced nimonics, boundary functions

NOMENCLATURE

A, B, D	Constants of integration	T	Temperature
c	Concentration	t	Time
C_p	Specific heat	U	Nondimensional concentration
G	Thermal gradient	Z	Decoupled solution variable
F_o	Fourier number	z	Axial coordinate
h	Heat transfer coefficient	a, K	Diffusivity
K	Thermal conductivity	(3)	Decoupling constant
L	Latent heat	ϕ	Porosity
m	Mass	TV	Similarity variable
R	Growth rate	X	Velocity of interface in similarity form (X and T) are identical)
r	Radial variable	T	Nondimensional time
s	Interfacial position ($s = 2\lambda\sqrt{\alpha_{12}\tau}$)	θ	Nondimensional temperature
		ρ	Density

1. INTRODUCTION

The art of controlled alloy solidification is not new. It appears that some controlled microstructures were used in the fabrication of Damascus steel. The iron pillar of Delhi and similar artefacts used unknown methods. Both may have been the result of repeated mechanical working and hot forming. These ancient arts have been lost but are being rediscovered- possible reconstructions of the processes have been described^{1,2}.

Eutectic alloys of low melting point can often be formed with lamellar or rod microstructure by the controlled freezing³. Unidirectionally solidified composites have been formed in this way, many by *in situ* processing⁴. The control of growth rate to regulate microstructures (lamellar, rod, spheroidal, cuboidal) has occupied material scientists and metallurgists from the advent of the steel age to that of advanced nimonics and superalloys. In contemporaneous alloy making, the breakdown of regular microstructures into Chinese script is well-known. Such transformations and properties were studied in detail for producing superior alloys for industry and military purposes. Phases of steel were extensively manipulated.

The importance of such materials led to a comprehensive study by NASA⁵ on microstructures of several superalloys. Processing parameters were found to control the stability of the interface and have been extensively studied in steel technology⁶.

While, earlier technologies used mechanical pre-treatment and post-treatment at elevated temperatures, later developments focused on controlled alloy solidification. The analysis of such moving boundary problems has posed problems due to their nonlinearity. The determination of the moving-phase boundary has been historically difficult to achieve, and solutions in the closed form are available in a very few cases^{7,9}. Recent theoretical and experimental work has been given by Loria^{10,12}.

In the finite difference numerical approach, the major difficulty is in the time-dependent and nonlinear boundary conditions like moving interface, and the irregular shape of the interface. Immobilisation

of the phase interface is a major step in the solution. Similarity transformations are one of the means of achieving such a goal. The moving interface is a time-dependent boundary condition. Very few exact solutions have been obtained^{13,14}. Mathematically, the time term introduces parabolicity into the otherwise elliptic nature of the problem, and in the numerical methods, several integration passes are required to arrive at the convergence. No doubt, numerical methods do exist for solution, but these lack the elegance of formal closed-form analytic solutions that reveal the nature of the type of solution involved.

In the Saitoh method⁷, a transform is used based on the boundary functions, with a jump condition across the interface. The boundary is immobilised by the transform. A variable mesh and variable time step is used to obtain a numerical scheme with a convergence criterion to fix the moving boundary position. Both the interface and the outer boundary can be treated in the transform. Various finite difference approaches are analysed⁸. In the fixed grid and the moving-phase boundary methods, the moving boundary is not explicitly considered in the finite difference solution.

Duda's⁸ convergence criteria are based on the convergence of the temperature profiles in the two slabs across the interface. Del Giudice⁹ used a finite element approach, with the Galerkin optimisation. Varying the specific heat, rather than a jump condition, approximates latent heat effects. Del Giudice mentions possible coupling of heat and mass transfer, but neglects mass transfer in the analysis. None of the earlier works have given solutions for coupled mass and heat transfer.

In the present work, an improvement over such methods is given. In particular, temperature and concentration are coupled. The convergence criteria use a mass and energy balance across the interface, with a solution for the eigenvalue X , which gives the boundary position coupled with time (related to the Fourier number). Furthermore, the interfacial temperature is not constant, and both interfacial temperature and concentration are computed, not assumed.

Nickel-based superalloys have been developed to have formable, high temperature corrosion-resistant and creep-resistant alloys. Popular alloys for aerospace applications include IN 718 (55 % nickel and 15 % iron), 625, and other variants. A peculiarity of IN 718 alloy is the large percentage of niobium and solvus transition range (75 K). The segregation of low melting point solutes like niobium is extremely difficult to remove by post-processing. Among such defects are freckles (niobium-rich segregates). The fabrication of defect-free large ingots of nickel superalloys remains a scientific and technological challenge. The present work has been carried out as a step forward in this direction.

2. ANALYSIS

A diffusional model is considered under temperature and concentration gradients with no pressure-assisted diffusion or gravity-assisted flow. A porous microstructure is assumed. It was proposed to look at different scenarios with types of boundary conditions—a cylindrical coordinate system with convective, Dirichlet, and heat-sink boundary condition, as also a porous half-space under Dirichlet boundary conditions, (the model used neglects certain physical constraints on the actual freezing). Among these are the cup-shaped bottom profile of the liquid pool, the coupling of z with r , and the finiteness of the outer radius).

The porosity parameter is a measure of the available volume for diffusion and includes the capillary pathways through which diffusion or transport occurs. The effect of the media is to provide pathways for the mass and heat transfer. The diffusivities and heat transfer parameters are the effective parameters and must be empirically determined for accurate predictions.

The following mathematical derivations are specific to the cylindrical system since the important application of defect-free ingot formation was motivating the work.

Assumptions Used

- (a) Porous media of uniform porosity e (porosity allows mass diffusion)
- (b) Saturated medium (in the sense that available mass does not change by adsorption or reaction)
- (c) Temperature of freezing not constant, can vary using additional equations (included in cases of slab freezing (Dirichlet and self-freezing).
- (d) Heat sink along the cylinder axis is of delta function type.

Boundary Conditions

The boundary conditions (nondimensional) are:

$$\text{Solid temperature } Q_2(\theta, t) = 0$$

Freezing at temperature θ_m (can be variable and solved for)

$$\text{Solid concentration, } t(\theta, T) = 0$$

$$\text{Final temperature } \theta_2 = 0$$

Initial Conditions

The Initial conditions are:

Initial molten liquid at temperature θ_0 (nondimensional)*

Here, U is the nondimensional concentration, θ is the nondimensional temperature, and r is the radial variable.

For the slab case, the normalisation is done wrt the triple-point values (fixed). Normalisation used is T/T_3 for Dirichlet and self-freezing.**

For the cylindrical case, the following conditions are used:

$$e = (r - r_0)/(T_0 - T_j)$$

$$U = 1 - C/C_0$$

* The dimensional values are denoted as T and c , subscript meanings remaining the same.

** Normalisation: $U = 1 - C/C_0$; $\theta = (T - T_0)/(T_e - T_m)$, where T_0 , C_0 are boundary temperatures and concentrations. Subscript 3 refers to triple-point values—considered fixed for any substance, whereas melting point values change with the equation of state.

The change of sign for temperature is to allow both curves for temperature and concentration to be plotted on the same graph.

Henceforth, the calculations are in dimensionless variables.

Subscripts

- 0 For reference (initial or boundary)
- 1 For liquid
- 2 For solid
- 3 Triple-state reference

Given below are the calculations specific to the cylindrical geometry. For the slab and self-freezing cases, the cylindrical operator is replaced with the appropriate form. Dirichlet boundary condition similar to the foregoing were used with similarity variable $TI = jt/2(ar)^{0.5}$.

Liquid Region

In the liquid region ($0 < r < s$)

$$39./aT = ajrd/dr (r\partial\theta_1/\partial r) \tag{1}$$

Solid Region

In the solid region ($s < r < \infty$)

$$39_2 / 9t = a_2/rd/dr (r\partial\theta_2/\partial r) + eL/pCp \partial U/\partial \tau \tag{2}$$

where

- a, Thermal diffusivity in region, i
- e Porosity (of the medium)
- p Density
- Cp Specific heat
- U Nondimensional concentration
- T Time
- L = Latent heat of transformation

$$(XT/r^2 = F_0 = \text{Fourier No.})$$

$$oc_{,2} = <x_{,}/a_2$$

The thermal properties are mainly those of the material pervading the pores, and due to this, the discontinuity occurs at the phase interface. The main contribution of the media is in allowing porosity and mass transfer. The second term in Eqn (2) describes the remelt effect due to solute rejection at the interface, also termed constitutional supercooling.

The equation for concentration is:

$$\partial U/\partial \tau = oc_m /r \partial^2 U/\partial r^2 \tag{3}$$

where $a_{...}$ is the mass diffusivity.

The above equations are a set of coupled diffusion equations with Dirichlet boundary conditions.

The solution is effected by means of the following decoupling variable:

$$3 [= 8L/pCp/(a_m-1)]$$

for cylindrical cases obtaining a new equation in terms of Z,

where

$$Z = 6_2 + \beta U \quad U = 1 - C/C_0 \tag{4}$$

Knowing the solution for c , the liquid phase temperature is decoded. The solutions are obtained in terms of Ei , the exponential integral function used by Paterson¹³ and also in Carslaw & Jaeger¹⁴. A Bessel series solution is also possible.

$$\text{Thus } dZ/dt = llr d/dr (rdZ/dr) \tag{5}$$

The solutions are obtained in terms of constants of integration A, and B, as follows:

In solid region

$$9_2 = Z - Pf/ = A_2 + B_2 Ei (-r^2/4t) - B_3 Ei (-r^2/4a_{m2}t) \tag{6}$$

$$\text{Applying } 9_2 (\infty, T) = 0, A_2 = 0$$

Liquid region temperature

$$6, = 6_0 + B_1 Ei(-r^2/4\alpha_{12}\tau) \quad (7)$$

Concentration solution

$$U = A_3 + B_3 Ei(-r^2/4\alpha_{m2}T) \quad (8)$$

Using the conditions: $A_2 = A_3 = 0$

$$5, = (6_n - 6_0)/Ei(-X^2)$$

$$5_2 = (0 + P_5 E_3 (-\alpha_{1m}\lambda^2)/Ei(-\alpha_{1m}\lambda^2) \quad (9)$$

Z_3 as shown below:

In addition, there is one more condition at the moving-phase interface which renders the problem nonlinear due to the discontinuity in properties:

Energy, balance

$$K_1 \partial\theta_1/\partial r - K_2 \partial\theta_2/\partial r = L (l-U)ds/di;$$

$$s = 2\lambda \sqrt{\alpha_{12}\tau} \quad (10)$$

Mass balance

$$a_{m2} JdU/dr = (l-U)ds/d-c \quad (U)$$

Convective Boundary Conditions

These boundary conditions are useful and appropriate when the boundary is cooled with flowing liquid or gas, such as in helium cooling of ingots. The same diffusional coupled system is posed, with the change that at $r = a$, the boundary, the radiation or convection boundary condition is satisfied. Hence

$$KdQ/dr \Big|_{r=a} = h_{\text{outer}}(0, -9_{\text{outer}}) \quad (12)$$

Solutions are obtained as before, the only difference being that A_2 need not to be zero. All other parameters are similar to the Dirichlet solution in form and value, excepting A_2 and B_2 .

Thus

$$A_1 = \theta_0$$

$$A_2 = kB_3/h[2 P/fl + hlk P Ei (<\mathcal{L})] - B_2klh [21a - hlk Ei (\mathcal{F})] \quad (13)$$

$$f_{i\tau} = (s_0 + P_J B J Z_i (-a_m X^2) - A J / E i (-a_{11} X^2) \quad (14)$$

$$B_3 = \alpha_{12}\lambda^2 / [\alpha_n W E i (-oc_{1m} X^2) - \alpha_{m2} \exp(-\alpha_{1m}\lambda^2)] \quad (15)$$

$$s = 2\lambda \sqrt{\alpha_{12}\tau}$$

O, \mathcal{F} are given as $-a^2/(4a_{m2}T)$ and $-a^2/(4r)$, respectively. #

Carslaw and Jaeger¹⁴ give another solution of a line sink of strength $g > a_0$ and claimed this to be the only known solution for the cylindrical freezing case. In addition, a constant freezing velocity solution is given^{13,14}. The Dirichlet and convective boundary condition solutions for the cylinder have not been found elsewhere, especially for coupled concentration and temperature.

3. HEAT SINK ALONG Z-AXIS SOLUTION

Here, a heat line source along z-axis having a delta function form occurs. In effect, there is a cylinder of solidifying, liquid or dendritic porous media and liquid. As an approximation, a disk of liquid may be chosen far away from the ends (ie, top and bottom of a cylinder), where radial variations only exist. However, there is an implicit coupling of r with z due to the presence of heat sink/source along the z-axis.

The same equations are setup as before, the only change in the boundary conditions being due to the heat sink Q at the origin.

$$\lim [27i r dQ/dr] = Q \sqrt{\alpha_{12}T} \quad (16)$$

For asymptotic time and large r , the Dirichlet and convective solutions are the same. Only for finite time or radii, when A_1 is not zero, is it possible to have control of the interface by variation of A_2 . Use of helium cooling is claimed to improve freckle resistance^{1MZ}. Clearly, the effect is through radial heat transfer, since the helium is a film surrounding the entire outer surface, improving the convective transfer at all z coordinates at the same radius a . Change in A_1 will affect the mass and heat balance at the phase interface.

$r \Rightarrow 0$

The solution for temperature is checked using the above relation.

The boundary conditions being

$$\theta_2(\infty, \tau) = 0$$

$$U(\infty, \tau) = 0$$

Initial Conditions

$$\theta(r, 0) = 0$$

$$U(r, 0) = 0$$

using the normalisation.

$$\theta = (T_r T_j / (T_0 - T_m))$$

$$U = 1 - C/C_0$$

Solutions are

Solid

$$0 = \theta_m + Q/4\pi [Ei(-r^2/4\alpha_{12}\tau) - Ei(-\lambda^2)] \quad (17)$$

Liquid

$$\theta_2 = Z - \beta U \quad (18)$$

$$Z = A Ei(-r^2/4T) \quad (19)$$

where

$$A = (\theta_m + |\beta \xi| Ei(-a_{1m} A^2)) / \xi j(-a_{12} A^2) \quad (20)$$

$$D = \alpha_{12} \lambda^2 / [\alpha_{12} \lambda^2 Ei(-\alpha_{1m} \lambda^2) - \llcorner_{m2} \exp(-a_{1m} X^2)] \quad (21)$$

$$s = 2\lambda \sqrt{\alpha_{12} \tau}$$

Explicitly

$$\theta_2 = AEi(-r^2/4i) - \beta DEi(-a_{1m} X^2) \quad (22)$$

(liquid region)

These equations are similar to the Dirichlet solutions for region 2. The region 1 solution (solid) is different because of the heat sink singularity.

For the cylindrical case, the temperature of transformation was kept fixed at the triple point or appropriate melting temperature. Further derivations are possible with a variable temperature but were not calculated here.

4. COMPUTATIONAL RESULTS

Direct comparison of the three cases is not possible, since Q leads to a discontinuity at the origin with low temperatures as $z \rightarrow 0$. On the other hand, the Dirichlet and convective solutions are identical in so far as the solid phase is concerned, and also the functional form of the liquid region solution. It was observed that since A_2 is an additive constant for the convective solution, the profile will be shifted depending on the sign of A_r . Comparing B_2 and B_3 , it may be seen that for large a and finite time, $A_2 = gB_3 + xB_2$

where

$$g = \beta Ei(\Phi)$$

$$x = Ei(\Phi) \quad (23)$$

Since the shapes are similar for the two cases, the temperature profile will be shifted along the family of curves corresponding to lower L as shown in the Fig. 1, implying that the interfacial position has moved to the right. Hence, faster freezing is expected from a mathematical analysis.

Presented below are some computational results on Dirichlet problems (slab) and the case of a heat sink along z -axis for a cylinder:

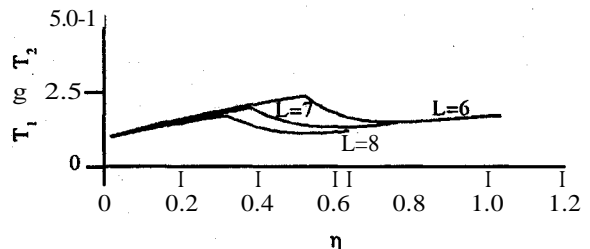


Figure 1. Temperatures for liquid and solid phases versus similarity variable η .

Case 1

Freezing of a semi-infinite slab half-space under Dirichlet boundary condition. A sample computational graph is shown as Fig. 1, with similarity variable TV as abscissa.

In the figure, the appearance of a zone of undercooling ahead of the liquid-solid interface is clearly seen. The profile as shown results from the extra remelt term in the diffusion equations. In actual fact, particles from the phase interface get detached and melt, causing a lowering of the liquid temperature by absorption of thermal energy as latent heat of melting. The interfacial temperature is solved for and not assumed constant. In nickel alloys containing niobium, this region will be a region of high niobium concentration, since niobium is a low melting point liquid and will be contained in the porous matrix of dendrites comprising earlier solidified components.

Case 2

In this scenario, solutions are depicted for a cylinder with a line sink of strength Q . Curves are shown superimposed for temperature and concentration for the three different values of L illustrating the change in freezing velocity as L is varied as shown in Fig. 2. Several other parametric variations have been attempted and successfully computed and plotted.

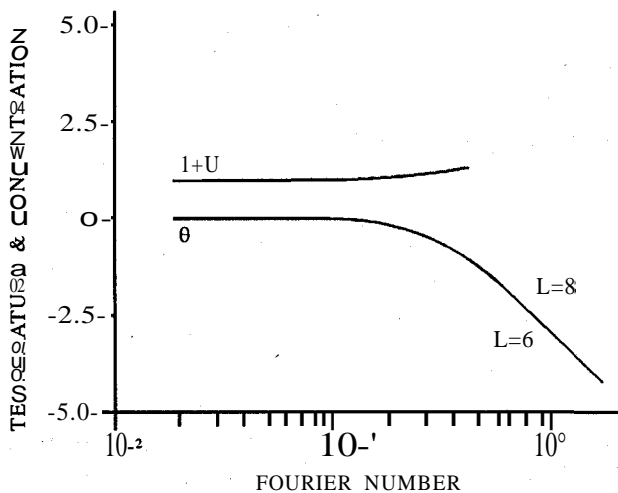


Figure 2. Temperature and concentration solutions versus Fourier numbers for cylinder with line heat sink, computed for various latent heat values.

Case 3

Here, a more complicated setup involving coupled freezing and sublimation is computed for the half-space, and results obtained for changes in the boundary temperatures and change in surface pressure. Figs 3 and 4 illustrate some of the variations. It may be seen that interfacial temperatures, concentrations, and pressures are variable (L as used in the figure refers to the sublimation latent heat). Equations of state are included for vapour and liquid transitions.

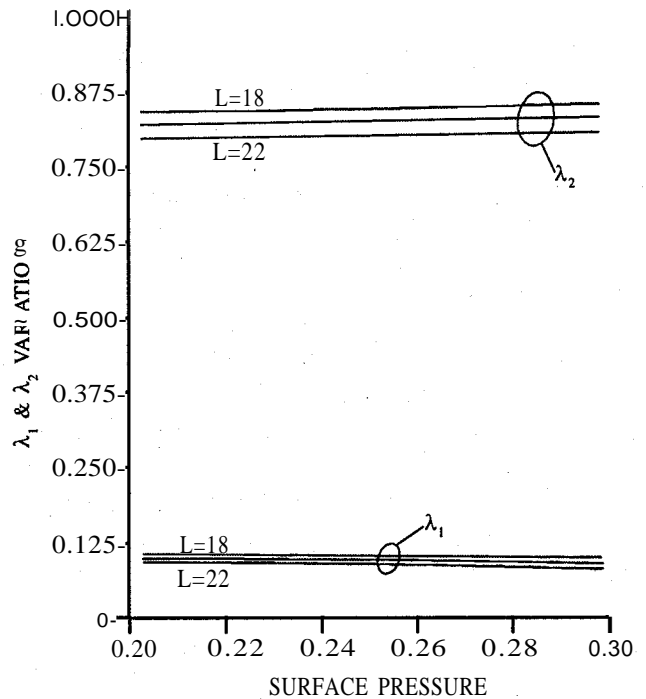


Figure 3. Freezing and sublimation solutions for self-freezing showing nondimensional velocity (eigenvalue 1) versus latent heat of sublimation and surface pressure.

5. COMPUTATIONAL METHOD

The solution is done using a decoupling constant P, which avoids the need to substitute the known solution for concentration and compute particular solutions. The simultaneous differential equations can also be solved with IMSL^s routines (simultaneous solvers), or by algebraic simplification. A secant solver or a bisection method can then be used to obtain the roots of the resulting transcendental equation. The secant method is fast and accurate

^s IMSL Commercial software package for engineering and scientific programmes. Many of the routines are listed in similar form¹⁷

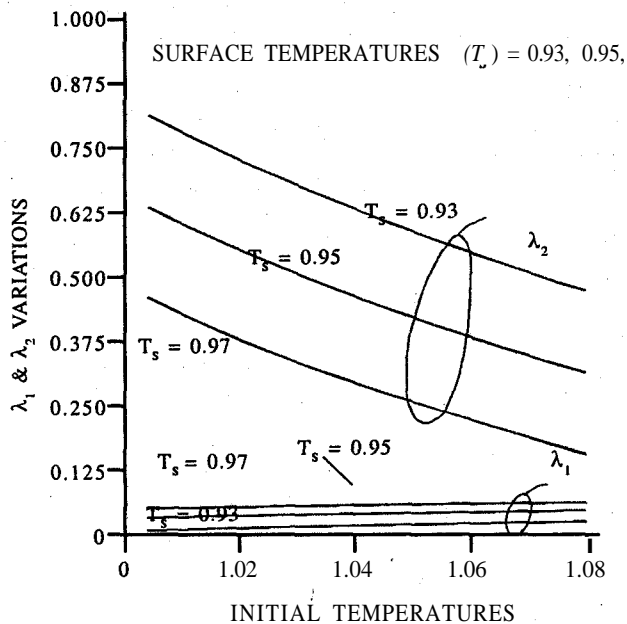


Figure 4. Freezing and sublimation curves for various surface temperatures and initial temperatures.

and avoids the need to compute Jacobians as in the gradient search methods. In this paper, Brent's technique has been used, outlined in Antia¹⁷. Zero finding routines use bisection with linear and inverse quadratic interpolations with specified tolerance and end limits¹⁷⁻¹⁹. A simultaneous solver used IMSL routines based on the Marquandt Levenberg minimisation method¹⁷ for the slab (Case 3, Fig. 4) with coupled sublimation and freezing¹⁹.

5.1 Interfacial Stability Criterion

Now to discuss another important issue, the stability criterion at the interface that controls the planar nature of the phase front.

In earlier physical metallurgy nomenclature, it is commonly seen as

$$GIR \gg AT/K \tag{24}$$

where

- G Thermal gradient
- R Freezing rate
- AT Undercooling
- K Thermal diffusivity

Let one examines the thermal energy balance at the moving interface:

Substituting for L, the actual heat in terms of temperature rise, specific heat, etc and using the earlier nomenclature, $G = dQ/dr$,

$$R = ds/dt, a = K/p Cp$$

Then, it is clear from Eqn (10), that

$$G/AT - G_2/R K/K, = AT/K, \tag{25}$$

The equation accounts for the thermal gradient effect in both the phases and gives a complete thermal balance, from liquid to solid. In addition, effects of porosity may be incorporated as e, and included by modifying the RHS of Eqn (10). The equation is linear in the terms G, AT! However, the form of the solution for temperature shows that these are exponential functions depending on radius squared, and in this sense, nonlinear. Moreover, the discontinuity in properties at the interface makes the problem inherently nonlinear^{17,20}.

It may be mentioned that in using the Fourier number F_0 , or $T = xl(ai)^5$ (in case of the half-space) as a dependent variable in analysing the figures, either time or distance can be fixed. In such cases, one may fix ones attention on the physical process at any point of time varying distance, or at a particular location as time progresses. The same figure applies to both the cases. Hence, if one positions oneself at the interface, by fixing $r = s$, the problem converts to a steady state problem in the sense that there is no change in the solution with time, as the profiles and conditions at the interface remain mathematically fixed (the interface may, of course, become unstable or other changes may occur with time, these cannot be predicted by the simplified model analysed here).

The physical basis for instability can arise from more than one cause. Physically, from a heat removal standpoint, as the radius of the solidifying ring increases, more area is involved, and hence, more latent heat available for removal. The easiest way for the alloy to accomplish the removal is by changing heat flux through a lowering of boundary

temperature or by increasing heat conduction. When such a mechanism is not immediately available, the surface of solidification can also provide large area by breaking up into facets, or form smaller new phase, such as freckles of lower melting point component like $NiNb_3$. Such an increase in area will then facilitate absorption of latent heat from the solidifying matrix to form liquid of $NiNb_3$ or other low melting point phase. Hence, remelt or supercooling should result, and in fact, does exist in many physical systems ahead of the phase interface.

5.1.1 *Effect of Boundary Conditions on the Rate of Freezing*

Direct comparisons are not possible for all scenarios; however, in a particular situation the variation of thermal parameters and boundary pressures, temperatures, and concentrations has been studied, with some results shown in the figures. For instance, a detailed study has been published for self-freezing⁹ (sublimation-driven freezing). Also, in the case of the porous semi-infinite cylinder discussed here, the effect of Dirichlet versus convective conditions have been qualitatively analysed. The convective condition has been applied industrially in the formation of superalloy ingots by cooling with helium gas on the periphery, thereby providing enhanced heat transfer and reducing defects in the ingot. In the case of the cylinder with a heat sink along the central axis, simulations show the effect of the conductivity and strength of the sink on freezing rate (A), together with other parameters.

The effect of the boundary conditions on the morphological stability of the interface occurs in an indirect way through the ability of the moving interface to be compatible with the heat and mass transfer gradients on either side of the interface. Often, the interface breaks up and a study was done by National Academy of Sciences and Engineering⁴ regarding optimum gradient parameters for many superalloys. The phase chemistry is also involved, so a purely physical and thermal/thermodynamic prediction cannot be given in a general manner. However, it is hoped that the foregoing study points the way to the general

directions to be taken and that some useful results are highlighted and reevaluated.

5.1.2 *Effect of Boundary Conditions & Thermodynamics on Undercooling*

The figure for slab freezing (linear half-space) shows a zone of undercooling ahead of the solidification front. Undercooling is well known to physical metallurgists, and is the driving force for progression of solidification. From a mathematical standpoint, it is caused by the appearance of the source term in the diffusion equation with temperature coupled with concentration. Without such a source term, the profile for T would follow the usual error function profile. However, due the terms combined with L , the dip in the T profile is caused by the additional L term. A smaller L will cause the interface to move faster. It may also happen that the profile may not be able to sustain a faster freezing rate because the thermal dissipation ahead of the freezing zone is insufficient to transport the energy away and maintain freezing. As a result, the interface breaks up. Alternatively, a change in freezing rate may cause a change in the shape of the undercooled profile. The freeezing rate may be modified due to a change in L , K , porosity, diffusivity or boundary temperatures. Also, the type of boundary condition can modify it.

5.1.3 *Effect of Buoyancy & Flow on Segregate Formation*

An earlier work by Copley²² has been visually illustrated convective jets and channeling in NH_4Cl , and it is recognised that it is a mechanism for segregate formation in cases where the vertical distance is substantial, especially in comparison with radial lengths. Recently, some papers have appeared attempting to link freckling with the buoyancy mechanism²³.

A simulation by Sung²⁴ using mesh spacing and effect of the vertical dimension indicates that the increase in the y coordinate appears to increase the segregation. Another recent publication²⁵ indicates that a critical Rayleigh number exists. The number is found to be 0.25 by experiment and is applicable to different alloy systems. A similar

study by Aubertin²⁶ shows that freckling is dependent on the Rayleigh number and also critically dependent on the growth front angle.

An overview²⁷ has appeared describing methods for reducing defects. The effect of the vertical ordinate in such studies appears in the coupling of the r and z coordinates via the curved phase interface and gravitational flow towards the centre of the ingot pool. This is, no doubt, a realistic model when the z coordinate or thickness of the ingot is substantial compared to the radius of the ingot.

By contrast, the present study focuses on the diffusive effects and thermal-mass coupling for one component, which can be extended to multicomponents and incorporate the chemical effects.

6. DISCUSSION

In earlier works, the steady state solution of a coupled heat and mass transfer problem was obtained for *in situ* composite formation with both r and z terms²⁰. A background research work on many such problems is given in Crank²¹.

Experimental results on actual vacuum arc remelt(VAR)-formed ingots of IN 718 indicate that freckle bands are formed in a ring at a certain radius. Helium cooling is claimed to eliminate freckling¹², whereas in ingots above a certain diameter, freckling has a greater tendency to occur. A solution, which comes to mind, is the effect of heat transfer in the radial direction. Due to the Lorenz forces and strong convective stirring, any fall in from electrode material is unlikely to form a radial band in the ingot.

The handle most often sought after by many researchers is the control of the mushy zone, where either interdendritic flow of niobium or solute rejection serves to concentrate niobium. The model discussed in this work illustrates the mushy zone and depression of the temperature profile graphically. One may thus picture such a zone around the phase-front in a radial ring and it is at some critical radius where the heat transfer balance is upset, that the

solute coalesces into freckles. The model also illustrates how helium cooling can affect the heat transfer balance by increasing the heat transfer through the matrix.

7. CONCLUSION

In the foregoing, an attempt has been made to present an alternative model based on convective channeling. Convective and buoyant effects may be appropriate for geometries where the vertical coordinate is substantial compared to the radial. In the present geometry (ingot formation), only a thin region remains liquid, forming an ingot disc over the already solidified regions. A small amount of gravity-assisted flow and microconvection may exist in cells, but it is doubtful if macroconvective currents, instigated by gravity and buoyancy, would persist in such a thin layer over a solid cylinder. For dendritic porous media, however, the macroscopic effects of buoyancy and circulation will be effective in local cells, not in a large region, as postulated by some. As such, it is likely that diffusive and chemical effects are predominant.

ACKNOWLEDGEMENTS

I would like to thank Dr Krishnan, Ex-Director, Gas Turbine Research Establishment (GTRE), Bangalore for his useful discussion. Also, I would like to thank Dr Boles of North Carolina State University (NCSU) where some earlier part of this work (heat sink and self-freezing models) was performed as part of PhD thesis under his guidance. The facilities of Triangle Universities Computational Centre (TUCC) and North Carolina State University Virtual Machine (NCSUVM) and computer time provided by the Mechanical Aerospace Engineering Dept of NCSU are acknowledged with thanks. I wish to thank DRDO for permitting me to publish this paper. Thanks to the referees for pointing out some relevant work and other aspects for improving the paper.

REFERENCES

1. Anantharaman, T. R. The iron pillar at Kodichadri in Karnataka. *Current Science*, 1999, 76(11), 1428-430.

2. Sherby, O. D. & Wadsworth, J. Damascus steels. *Scientific American*, 1985, 94-99.
3. Smallman, R. E. Modern physical metallurgy, Ed. 3. Butterworths ELBS, London, 1970.
4. Proceedings of International Conference on *in situ* Composites, Lakeview, Conn., 1972. National Academy of Sciences and Engineering. Reported by NMAB. Report No. NMAB 308.1,2,3, 1973.
5. Lemkey, F. D. & McCarthy, G. Quaternary and quinary modifications of eutectic alloys strengthened by delta Ni^{Cb} lamellae and gamma prime Ni^{Al} ppts. NASA, Washington DC, 1975. Report No. NASA-CR-134678.
6. Hume Rothery, W.¹ The structure of alloys of Iron. Pergamon, UK, 1969.
7. de Giudice, S.; Comini, G. & Lewis, R.W. Finite element simulation of freezing processes in soils. *Int. J. Num. Anal. Meth. Geomech.*, 1978, 2, 223-35.
8. Duda, J. L.; Malone, M.F.; Notter, R. H. & Vrentes, J.S. Analysis of two-dimensional diffusion-controlled moving boundary problems. *Int. J. Heat Mass Transfer*, 1975, 18, 901-10.
9. Saitoh, T. L. Numerical methods for multi-dimensional freezing problems in arbitrary domains. *J. Heat Transfer*, 1978, 100, 294-99.
10. Loria, E. A. (Ed) Superalloy 718, metallurgy and applications. The Minerals Metals and Materials Society, Warrendale, Pa, USA, 1989.
11. Loria, E. A. (Ed) Superalloy 718, 625, and various derivatives. The Minerals Metals and Materials Society, Warrendale, Pa, USA, 1991.
12. Loria, E. A. (Ed) Superalloy 718, 625, 706 and various derivatives. The Minerals Metals and Materials Society, Warrendale, Pa, USA, 1994.
13. Paterson, S. Propagation of boundary effusion. *Glasgow Math Assoc. Proc.*, 1952, 1, 42-47.
14. Carslaw, H. S. & Jaeger, J. C. Conduction of heat in solids, Ed. 2. Clarendon Press, Oxford, 1959.
15. Schlatter, R. Effect of cooling on VAR. ingot quality of 718. In TMS Conference, Superalloys 718, 625, 706 and various derivatives, edited by E. A. Loria. The Minerals Metals and Materials Society, Warrendale, Pa, USA, 1994.
16. Hosamani, L.G.; Wood, W. E. & Devletian, J. H. Solidification of alloy 718 during VAR with helium gas cooling between ingot and crucible. In Proceedings of the first International Symposium on Metallurgy and Application of Alloy 718. The Metals Society, 1989. pp. 49-57.
17. Antia, H. M. Numerical methods for scientists and engineers. Tata McGraw Hill, Bombay, 1991.
18. Brent, R. P. Algorithms for minimisation without derivatives. Prentice Hall, New Jersey, USA, 1973.
19. Basu, R. D. & Boles, M. A. Self-freezing in a porous medium with unknown interfacial conditions. *Int. J. Energy Res.*, 1994, 18, 449.
20. Yue, A. S.; Basu, R. D. & Yang, T. T. On a theory of fibre thickening. In Proceedings of International Conference on *in situ* Composites, NMAB 308.1, National Academy of Sciences and Engineering (NAS), Washington DC, 1973. pp. 75-86.
21. Crank, J. Free and moving boundary problems. Clarendon Press, Oxford, 1984.
22. Copley, S.M.; Giamei, A. F.; Johnson, S. M. & Hornbecker, M. F. The origins of freckles in unidirectionally solidified castings. Pratt and Whitney Aircraft, Middletown, Conn., 1969. Advanced Materials Research. Laboratory, Development Report, 19, No. 69-028.
23. Gu, J. P.; Beckerman, C. & Giamei, A. F. Motion and remelting of dendrite fragments during unidirectional solidification of a nickel-based superalloy. *Metallurgical Transactions A*, 1997, 28A, 1533-542.
24. Sung, P. K.; Poirier, D. R. & Felicelli, S. D. Sensitivity of mesh spacing on simulating

- macrosegregation during directional solidification of a superalloy. *Intl. J. Numer. Methods Fluids*, 2001, 35(3), 352-70.
25. Beckerman, C.; Gu, J. P. & Boettinger, W. J. Development of a freckle predictor via Rayleigh number method for single crystals. *Met. Matls. Trans.*, 2000, 31A(10), 2545-557.
26. Aubertin, P.; Wang, T.; Cockroft, S. L. & Mitchell, A. Freckle formation and freckle criterion in superalloy castings. *Met. Matls. Trans.*, 2000, 31B(4), 801-11.
27. Van Den Ayle, J. A.; Brooks, I. A. & Powell, A. C. Reducing defects in remelting processes for high performance alloys. *Journal of Metals*, 1998, 50(3), 22-25.

Contributor



Dr Rahul Basu obtained higher qualifications and underwent coursework at RTF, USA, on leave from DRDO during-1985-91. During this time, he received training in the areas of mathematics, materials and engineering sciences, computer simulation using advanced computers. Much of the computer work described here was completed on supercomputers at the Triangle Universities Consortium at RTF, NC, with computations and graphical output in one integrated package developed by him. The doctoral thesis was approved for candidacy in 1989. After returning from USA in 1991, he worked as Senior Scientist at the Gas Turbine Research Establishment (GTRE), Bangalore and worked on the problem of freckling in superalloys which was apparent in large ingots of IN718, etc.